

## A METHOD FOR MAPPING THE TEMPERATURE PROFILE OF X-RAY CLUSTERS THROUGH RADIO OBSERVATIONS

GILBERT P. HOLDER AND ABRAHAM LOEB<sup>1</sup>

Institute for Advanced Study, Einstein Drive, Princeton NJ 0854 085400

*to be submitted to ApJL*

### ABSTRACT

Many of the most luminous extragalactic radio sources are located at the centers of X-ray clusters, and so their radiation must be scattered by the surrounding hot gas. We show that radio observations of the highly-polarized scattered radiation (which depends on the electron density distribution) in combination with the thermal Sunyaev-Zeldovich effect (which measures the electron pressure distribution), can be used to determine the radial profile of the electron temperature within the host cluster. The sensitivity levels expected from current instruments will allow radio measurements of mass-weighted cluster temperature profiles to better than a  $\sim 1$  keV accuracy, as long as the central radio source is steady over several million years. Variable or beamed sources will leave observable signatures in the scattered emission. For clusters with a central point source brighter than  $\sim 1$  mJy, the scattered polarization signal is stronger than competing effects due to the cosmic microwave background.

*Subject headings:*

### 1. INTRODUCTION

Massive galaxy clusters often host a bright radio source at their center (e.g., Zhao, Burns & Owen 1989). A small fraction of the radiation emitted by the central source is expected to scatter off the surrounding intracluster electrons and obtain a high level of polarization. The radial profile of the scattered radiation depends only on the electron density distribution within the cluster, in difference from the thermal Sunyaev-Zeldovich (SZ) effect which depends on the electron pressure distribution (see Carlstrom, Holder & Reese 2002 for a recent review). In this *Letter*, we show that the temperature profile of the intracluster gas can therefore be determined by means of radio observations alone, through the combined detection of the polarized scattered light from a central source and the SZ effect. This method for inferring cluster temperatures is particularly powerful for distant clusters, where the alternative option of using an X-ray telescope requires very long integration times and is less practical.

The typical optical depth for Thomson scattering through the core of massive X-ray clusters is  $\sim 0.01$  (Mason and Myers 2000), and so roughly a percent of the observed flux from the central radio source should appear in the form of a diffuse radio halo around it. To give a concrete example, a point source observed to have a flux density of 1 Jy in a cluster at a redshift  $\sim 0.2$  would generate a  $\sim 10$  mJy radio halo on an angular scale of  $\sim 1'$ , assuming it is emitting isotropically. Despite its faintness, the diffuse radio halo could be separated from contaminating sources due to the high amplitude ( $\sim 50\%$ ) and the large-scale tangential alignment of its polarization pattern (Sazonov and Sunyaev 1999; Sunyaev 1982; Sunyaev and Zeldovich 1980). The typical intrinsic polarization of individual point sources is only a few percent, making the central point source a much less significant contaminant in the polarization

map than it is in the intensity map. With current instruments such as the VLA achieving stability over a dynamic range of  $10^5$  (Perley 1999), the halo signal should be detectable.

Several groups are currently constructing radio telescopes optimized to search for the SZ signature of clusters of galaxies (e.g., Carlstrom, Holder & Reese 2003). The planned SZ surveys will be efficient at finding clusters of galaxies up to relatively high redshifts ( $z \sim 1$ ), from which the received X-ray flux would be weak. In addition to the reduction in the X-ray flux due to the large cosmological distance, the prominence of galactic outflows (due to star formation and quasar activity) at  $z \sim 1 - 2$  will likely disperse somewhat the intracluster gas and make the cluster less X-ray luminous (Evrard and Henry 1991; Kaiser 1991). These problems are not nearly as acute for SZ observations (Holder and Carlstrom 2001), raising the possibility of strong SZ sources that are difficult to follow up with X-ray telescopes. Our proposed method provides an important alternative route to probing the density and temperature distributions of the intracluster gas in the most massive clusters that will be discovered by future SZ surveys.

Most SZ-detected clusters will probably not have a suitable central point source for obtaining detailed images of the reflected images. In nearby clusters, roughly one quarter of clusters host a radio source with radio power greater than  $10^{24.5}$  W/Hz at a wavelength of 21 cm (Ledlow and Owen 1995). At  $z \sim 0.5$  this corresponds to roughly 10 mJy, so it might be expected that the polarized emission might be detectable in a sizable fraction. However, the observed radio luminosity function (Ledlow and Owen 1996) at high power falls off quickly ( $dN/d\ln P \propto P^{-1.5}$ ), so the fraction of sources with high enough radio powers to give a strong signal is likely a few percent, depending on how much the cluster radio source luminosity function evolves with redshift. From recent observations at 30 GHz (see Bennett et al. 2003 for a recent compilation) of radio point sources, one would expect roughly 300 sources brighter than 0.1 Jy per stera-

Electronic address: holder@ias.edu

<sup>1</sup> Guggenheim Fellow; on sabbatical leave from the Astronomy Department, Harvard University.

dian. Deep SZ surveys expect roughly 30000 sources per steradian (Carlstrom *et al.* 2002), so if every bright radio source is embedded in a cluster the reflected emission should be significant for roughly 1% of detected SZ clusters.

The projected profile of the scattered radio emission is a direct probe of the electron density run with radius  $n_e(r)$ . By comparison, the X-ray emissivity is sensitive mainly to  $n_e^2$ , while the SZ effect probes  $n_e T$ , where  $T(r)$  is the radial profile of the electron temperature. The combination of SZ measurements with radio polarization measurements allows a direct determination of the electron temperature profile, while the combination of X-ray observations with polarization halo measurements allows a direct distance determination, based on the same method that is currently used with X-ray and SZ observations (Reese *et al.* 2002). Finally, the combination of X-ray, SZ, and polarization observations would allow a consistency check on the underlying simplifying assumptions, such as the spherical geometry of the cluster or the steadiness of the central source.

Our proposed method could be complicated by temporal variability of the radio source, because of the geometric time delay that the scattered light acquires. Images of extended radio jets indicate that extended radio sources are often stable over those timescales (Begelman, Blandford, and Rees 1984). However, if central cluster sources do vary on short timescales, then an independent mapping of the electron distribution around these sources (e.g. based on deep X-ray observations) could be used to read off their temporal variability as a function of age from the brightness distribution as a function of projected radius in their scattered radio surface brightness. If the source is strongly beamed in a direction not aligned with our line of sight, it is possible to use the reflected emission as a probe of both the source luminosity and the surrounding medium (see, for example Chiaberge *et al.* 2003 for an application using X-ray and ultraviolet imaging). However, for simplicity, we focus in this publication on the subject of steady sources emitting isotropically.

In §2 we calculate the polarization of the scattered radio halo, while §3 outlines a synthetic observational procedure to test the prospects for temperature measurements by the above method. We close with a discussion of some observational and theoretical hurdles which must be overcome as well as a summary of the many potentially important applications of measuring diffuse radio polarization in galaxy clusters.

## 2. SCATTERED RADIO HALO AROUND A CENTRAL POINT SOURCE

We start with the idealized case of a steady point source of observed spectral flux density  $S_\nu$  and spectral luminosity  $L_\nu$  (per observed frequency  $\nu$ ) at the center of a spherical cluster. We define a coordinate system centered on the cluster with the  $z$ -axis along the line of sight and calculate the circularly symmetric brightness profile of the scattered radiation. An infinitesimal cell of physical area  $dxdy$  on the sky contains  $dN_e = n_e dxdydz$  electrons and therefore has a physical effective cross-section to incoming photons of  $dN_e \sigma_T$ , where  $\sigma_T$  is the Thomson cross section. The total spectral luminosity that will therefore be scattered by this cell is  $dN_e (\sigma_T / 4\pi r^2) L_\nu$ ,

where  $r$  is the 3D radius from the cluster center. The radiation scattered along the  $z$ -axis toward the observer will be preferentially polarized in the direction perpendicular (on the sky) to the cylindrical radius vector. This is particularly easy to see for a parcel of electrons located in the plane of the sky but offset from the central source. An initially unpolarized source will have equal components of the electric field  $\mathbf{E}$  oriented in the plane of the sky (perpendicular to the radius vector) and along the  $z$ -axis. Scattering of the  $z$ -polarized photons into our line of sight will be suppressed, leading to the scattered radiation being completely polarized in the direction perpendicular to the radius vector in the plane of the sky. In general, the suppression factor of the component along the cylindrical radius vector is proportional to  $\cos^2 \theta$ , where  $\theta$  is the angle between the spherical radius vector and the  $z$ -axis.

Defining an azimuthal angle on the sky  $\phi$  and a coordinate system for the Stokes parameter  $Q$  (in units of intensity, not flux) such that the maximum of  $Q$  is obtained at  $\phi = 0$ , we find (see also Sazonov & Sunyaev 1999, Sunyaev 1983) that for a general distribution of electron number density  $n_e(\vec{r})$

$$Q(R, \phi) = \frac{3\sigma_T}{16\pi} \left( \frac{S_\nu}{\text{Jy}} \right) \cos 2\phi \int_{-\infty}^{+\infty} dz \frac{d_A^2 R^2}{r^4} n_e(R, \phi, z) \frac{\text{Jy}}{\text{sr}}, \quad (1)$$

where  $R$  is the cylindrical physical (not angular) radius in the plane of the sky,  $r = \sqrt{R^2 + z^2}$ , and  $d_A(z)$  is the angular diameter distance to the source (arising here from the conversion of physical area on the sky,  $dxdy$ , to solid angle).

For an electron number density profile following the “ $\beta$ -profile”, where  $n_e = n_{e0}(1 + r^2/r_c^2)^{3\beta/2}$  (Cavaliere and Fusco-Femiano 1976), one obtains for the Stokes  $Q$  parameter [see, Gradshteyn & Ryzhik 1980, 3.259(3), p. 299]

$$Q(R, \phi) = \frac{3\sigma_T}{16\pi} \left( \frac{S_\nu}{\text{Jy}} \right) \cos 2\phi \frac{d_A^2}{R^2} \frac{n_{e0} r_c}{(1 + R^2/r_c^2)^{(3\beta-1)/2}} \times {}_2F_1\left[2, \frac{1}{2}; \frac{3}{2}\beta + 2; 1 - \frac{r_c^2 + R^2}{R^2}\right] \times B\left[\frac{1}{2}, \frac{3}{2}(1 + \beta)\right] \frac{\text{Jy}}{\text{sr}}, \quad (2)$$

where  $B(x, y)$  is the Beta function and  ${}_2F_1(a, b; c; z)$  is the hypergeometric function. A similar expression in terms of a Beta function and  ${}_2F_1$  can be obtained for the total scattered intensity. For the case of  $\beta = 3/2$  an explicit expression can be found in Sunyaev (1983). Note that the source redshift does not enter explicitly into this expression, since the intrinsic source luminosity and reflected luminosity share the same redshift factors.

Typical parameter values are  $d_A \sim 1 h^{-1} \text{Gpc}$  for a source at a cosmological distance, and  $n_e \sim 0.01 \text{cm}^{-3}$ ,  $r_c \sim 150 h^{-1} \text{kpc}$  for typical cluster cores. For a 1 Jy source, these parameters correspond to roughly 1 mJy/arcmin<sup>2</sup> at about a core radius ( $\sim 0.5'$ ) from the central source. At an observing frequency of  $\nu = 30 \text{GHz}$ , the relevant conversion to brightness temperature is 1 Jy/arcmin<sup>2</sup> = 0.4 K, and so the scattered intensity is equivalent to nearly a mK polarized temperature signal. In a signal-to-noise sense, this is an easy signal to detect for the current generation of instruments. The difficulty is that such a signal arises from a field that by construction has a 1 Jy source at the center which must

be stably removed. Typically, the 1 Jy source may also intrinsically produce tens of mJy of polarized flux. Note that the polarized scattered radiation will be more centrally concentrated than the projected gas distribution due to the  $1/r^2$  fall off of the source flux as seen by the cluster electrons.

### 3. PROSPECTS FOR TEMPERATURE MEASUREMENTS

We examine the feasibility of temperature measurements by constructing synthetic observations of galaxy clusters with steady point sources embedded at the center and emitting isotropically. We first use  $\beta$ -models and then examine clusters in three-dimensional cosmological simulations with hydrodynamics. Throughout our discussion, we consider a 1 Jy source observed at 30 GHz. All properties of the polarized radio halo, scale directly with the point source flux. The scattered intensity from the point source may exceed the SZ signal amplitude in the core of the cluster. In principle, high-frequency SZ observations are not necessary, since the scattered intensity can be reconstructed from the polarization and removed from the SZ flux.

First we assume a  $\beta$ -profile for the radial profiles of the gas temperature and density, and construct the brightness profiles for the SZ effect and polarized radio halo around the central source. Rather than tailor our predictions closely to a particular instrument, we assume that instruments such as SZA<sup>2</sup>, CARMA<sup>3</sup>, AMI<sup>4</sup>, Amiba<sup>5</sup>, EVLA<sup>6</sup>, or ALMA<sup>7</sup> may generically be thought of having sensitivity to a range of angular scales from roughly arcsecond scales up to a few arcminutes with up to  $\mu\text{K}$  sensitivity. Note that SZA and AMI are not currently planned to be used for polarization studies, but it would not be difficult to adapt these instruments for polarization studies.

The details will depend crucially on the observing frequency. In general, large scale emission will be filtered out. We assume that this filtering is on a scale of ten arcminutes or a radius in the  $u-v$  plane corresponding to  $\sim 300$  wavenumbers (in units of the observing wavelength) and that there is no sensitivity to larger scales (i.e., we assume a high pass filter). At cm to mm wavelengths this is effectively required to avoid contamination from primary cosmic microwave background (CMB) anisotropies. In addition, high angular resolution is required to isolate the central point source. We assume a maximum  $u-v$  radius of 3000 wavenumbers and an equal noise contribution per  $\log$  interval in  $u-v$  radius between the above inner and outer cutoffs. Noise was added such that the resulting noise in each map was  $1 \mu\text{K}$  and beam effects were ignored. An observing frequency in the Rayleigh-Jeans was assumed for the SZ component.

We assumed a  $\beta$ -profile for each of the electron number density profile and the pressure profile, with a central electron number density of  $0.01 \text{ cm}^{-3}$ , a central temperature of  $T_{e0} = 5 \text{ keV}$ , a common core radius of  $0.75'$  for both  $n_e(r)$  and  $T(r)$ ,  $\beta_e = 2/3$  for the electron density profile and  $\beta_P = 1$  for the pressure profile. The cluster

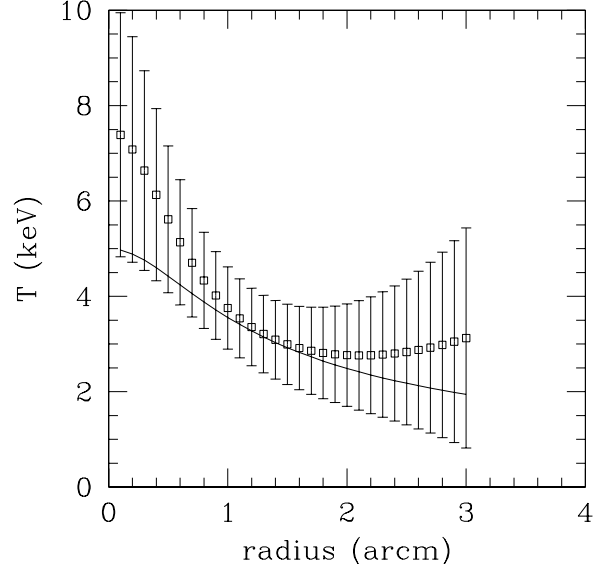


FIG. 1.— Reconstructed temperature profile for a single realization (assuming the electron density and temperature profiles are both  $\beta$ -models) with approximate  $1-\sigma$  uncertainties. Neighboring points are highly correlated. The true input profile is shown as a solid line.

was assumed to be at  $z = 0.5$ . A realization of “data” was generated and then fit to a model with two  $\beta$ -models, with the centers of the profiles constrained to be at the cluster center. Each  $\beta$ -model had three parameters, and the presence of a point source at the center was allowed in terms of two free parameters (flux and polarized flux). A Markov chain Monte-Carlo method was used to estimate constraints on the temperature profile as a function of radius. Specifically, random steps were taken in the 8-D parameter space and accepted if the proposed point was higher probability or rejected according to a probability set by how less likely the proposed point was than the current point. After many samples, the list of points in the chain provides a sampling of the likelihood function. For each point in the chain the temperature profile  $T(r)$  was constructed. The resulting distribution of temperature profiles is shown in Figure 1, where all parameters have effectively been marginalized over. There is a dramatic reduction in the uncertainties if the central point source flux is assumed to be known both in terms of polarized emission and the SZ signal; this simply reflects the fact that the polarized intensity is highly concentrated, and therefore can be partially mimicked by a point source. Given the importance of the central flux it seems prudent to simply marginalize over the unknown flux and accept that the temperature uncertainties will be on the order of  $\sim 1 \text{ keV}$ , comparable to X-ray spectroscopic temperature uncertainties.

Real clusters are unlikely to follow ideal spherically-symmetric  $\beta$ -profiles, and so we repeated the calculation for clusters extracted from numerical simulations produced by the Hydra Consortium<sup>8</sup> and made publicly

<sup>2</sup> <http://astro.uchicago.edu/SZE/survey.html>

<sup>3</sup> <http://www.mmarray.org>

<sup>4</sup> <http://www.mrao.cam.ac.uk/telescopes/ami>

<sup>5</sup> <http://www.asiaa.sinica.edu.tw/amiba>

<sup>6</sup> <http://www.aoc.nrao.edu/evla>

<sup>7</sup> <http://www.alma.nrao.edu/>

<sup>8</sup> <http://hydra.susx.ac.uk>

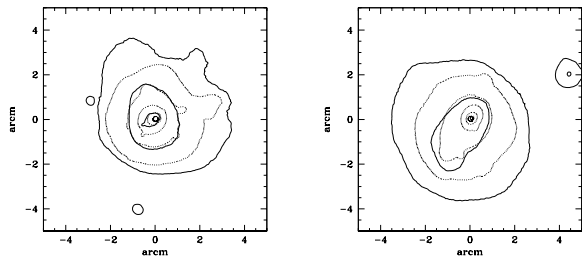


FIG. 2.— Maps of thermal SZ (solid) and polarized intensity (dotted) for the most massive (left) and second most massive (right) clusters in the simulation archive. Outermost contours are  $1 \mu\text{K}$  at 30 GHz and they increase in factors of 10 inward. The polarized intensity assumes a central 1 Jy source, and that the conversion to temperature units is  $1 \mu\text{K}$  for  $0.43 \mu\text{Jy}$  per square arcminute. The direction of polarization at each point is tangential to the cluster center.

available by the Virgo Consortium<sup>9</sup> on the web. The simulation data shows deviations from the ideal  $\beta$ -profiles that are expected in nature. These simulations have been used (da Silva *et al.* 2000) to study the statistics of SZ maps. Maps of two clusters, both in SZ and polarized emission, are shown in Figure 2. We repeated the above calculation, generating synthetic data, fitting to two  $\beta$ -profiles and comparing to the true temperature profile. Results were qualitatively similar to those for the case of the spherical  $\beta$  clusters. In the simulated clusters the mass-weighted temperature within three arcminutes was recovered with statistical errors of roughly 1 keV.

We have not attempted a detailed search to optimize the spatial sensitivity or frequency coverage. Contaminating and confusing sources will be less or more important at different spatial scales or observing frequencies. At low frequencies there could be confusion with diffuse synchrotron emission by the cluster or extended jet structures, while higher frequencies will run into both a relative dearth of very bright central point sources and dust emission from our Galaxy as well as distant star-forming galaxies (Fischer and Lange 1993).

#### 4. DISCUSSION

We have shown that radio measurements alone can be used to reliably measure temperature profiles of the gas in X-ray clusters. The current generation of radio instruments is already sufficient in terms of sensitivity, but the presence of a 1 Jy source in the center of the field will no doubt make sub-mJy polarized studies challenging. With the VLA performing at dynamic ranges exceeding  $10^5$  (Perley 1999), it is clear that the presence of the central source does not pose an inherent limitation to our method.

With typical scattered fluxes of  $\sim 1\%$  of the central source flux, it can be expected that the polarized scattered emission will exceed the  $\mu\text{K}$  level for all central sources brighter than about 1 mJy at 30 GHz. This is brighter than the *peak* emission due to the cluster scattering of the primary CMB quadrupole, which is itself significantly larger than any anisotropies due to thermal or kinetic SZ effects (Sazonov and Sunyaev 1999). A central point source is by far the single largest source of

a quadrupole anisotropy in the radiation field for many clusters at radio frequencies. Therefore, detection of the scattered radio halo could provide an intermediate target for an attempt to measure these smaller signals. To the extent that the radio spectrum is constant over the age of the source, the spectrum of the polarized emission should be the same as that of the central source, providing an important consistency check.

The nearly circular polarization pattern should provide a simple template for improving the detectability of the signal, and the compact angular scale implies that the CMB anisotropy is not a serious contaminant. Many clusters show signs of radio halos or radio relics (Giovannini and Feretti 2002). These generally have steep spectra, so it may be difficult to observe the polarized emission reflected from the central source at wavelengths longer than a few cm. Jets associated with the central source may be significant in the inner arcseconds. The largest contaminant will likely be the systematic problem of removing the very bright central source sufficiently accurately and stably so that it would not affect the measurements in the entire image.

Nearby clusters are too large (in angular size) to have a significant surface brightness so the studies considered here are probably most suitable for clusters at redshifts  $z \gtrsim 0.2$ . For studies of the SZ effect it should be noted that all sources above  $\sim 1$  mJy will contaminate the immediate vicinity of the point source at  $\mu\text{K}$  levels and therefore point source removal must be handled carefully. If bright radio sources are significantly beamed, then some radio SZ observations could be contaminated by this reflected emission even for sources that do not appear to be very luminous.

While we have outlined the potential for measuring temperature profiles, an equally exciting application would be to measure the time evolution of the radio flux from the central source. With cluster radii of roughly 1 Mpc the light travel times are a few million years. With  $\mu\text{K}$  sensitivities to polarized emission it will be possible to measure the age of the central source by simply finding an edge to the polarized emission; with independent temperature measurements, either from SZ spectral studies or X-ray spectroscopy, it would be possible to measure the time evolution of the central radio source. Surfaces of scattering corresponding to constant central source emission time are paraboloids (Sazonov and Sunyaev 2003), and so a good mapping of the three-dimensional electron distribution will be necessary.

In summary, the extremely high sensitivity and stability of current and near-future instruments should enable the use of the intracluster medium as a reflection nebula around bright point sources. This should provide some insight about the geometry of merging subclumps and a measure of the cluster electron density distribution in addition to the important applications outlined above. The observations present some unique challenges, but the potential scientific rewards are compelling.

G.P.H. is supported by a W.M. Keck Fellowship. A.L. acknowledges support from the Institute for Advanced Study at Princeton and the John Simon Guggenheim Memorial Fellowship. This work was also supported in part by NSF grants AST-0071019, AST-0204514 and

<sup>9</sup> <http://virgo.sussex.ac.uk/clusdata.html>

NASA grant NAG-13292 (for A.L.). We thank the Hydra and Virgo consortia for making their simulation products

publicly available in an accessible format.

#### REFERENCES

- Begelman, M. C., Blandford, R. D., and Rees, M. J. 1984, *Reviews of Modern Physics*, **56**, 255–351.
- Bennett, C. *et al.* 2003, *ApJ*, submitted, astro-ph/0302208.
- Carlstrom, J. E., Holder, G. P., and Reese, E. D. 2002, *ARA&A*, **40**, 643–80.
- Cavaliere, A. and Fusco-Femiano, R. 1976, *A&A*, **49**, 137.
- da Silva, A. C., Barbosa, D., Liddle, A. R., and Thomas, P. A. 2000, *MNRAS*, **317**, 37.
- Evrard, A. and Henry, J. 1991, *ApJ*, **383**, 95.
- Fischer, M. L. and Lange, A. E. 1993, *ApJ*, **419**, 433.
- Giovannini, G. and Feretti, L. 2002. Diffuse Radio Sources and Cluster Mergers: Radio Halos and Relics. In *ASSL Vol. 272: Merging Processes in Galaxy Clusters*, pages 197–227.
- Gradshteyn, I. S. and Ryzhik, I. M. 1980. *Table of Integrals, Series and Products*. Academic Press, New York, NY, USA.
- Holder, G. P. and Carlstrom, J. E. 2001, *ApJ*, **558**, 515.
- Kaiser, N. 1991, *ApJ*, **383**, 104.
- Ledlow, M. J. and Owen, F. N. 1995, *AJ*, **109**, 853–873.
- Ledlow, M. J. and Owen, F. N. 1996, *AJ*, **112**, 9+.
- Mason, B. S. and Myers, S. T. 2000, *ApJ*, **540**, 614–633.
- Perley, R. A. 1999. High Dynamic Range Imaging. In *ASP Conf. Ser. 180: Synthesis Imaging in Radio Astronomy II*, pages 275–+.
- Reese, E. D., Carlstrom, J. E., Joy, M., Mohr, J. J., Grego, L., and Holzappel, W. L. 2002, *ApJ*, **581**, 53–85.
- Sazonov, S. Y. and Sunyaev, R. A. 1999, *MNRAS*, **310**, 765.
- Sazonov, S. Y. and Sunyaev, R. A. 2003, *A&A*, **399**, 505–509.
- Sunyaev, R. A. 1982, *Soviet Astronomy Letters*, **8**, 175–+.
- Sunyaev, R. A. and Zeldovich, Y. B. 1980, *MNRAS*, **190**, 413.
- Zhao, J., Burns, J. O., and Owen, F. N. 1989, *AJ*, **98**, 64–107.